




RESEARCH ARTICLE

Higher reliability and validity of Wavelet-ALFF of resting-state fMRI: From multicenter database and application to rTMS modulation

Juan Yue^{1,2,3,4} | Na Zhao^{2,3,4,5,6} | Yang Qiao^{2,3,4,6,7} | Zi-Jian Feng¹  |
 Yun-Song Hu^{2,3,4} | Qiu Ge^{2,3,4} | Tian-Qing Zhang⁸ | Zhu-Qian Zhang⁸ |
 Jue Wang⁹  | Yu-Feng Zang^{2,3,4} 

¹TMS Center, Hangzhou Normal University Affiliated Deqing Hospital, Huzhou, China

²Center for Cognition and Brain Disorders, The Affiliated Hospital of Hangzhou Normal University, Hangzhou, China

³Institute of Psychological Sciences, Hangzhou Normal University, Hangzhou, China

⁴Zhejiang Key Laboratory for Research in Assessment of Cognitive Impairments, Hangzhou, China

⁵Unit of Psychiatry, Department of Public Health and Medicinal Administration, & Institute of Translational Medicine, Faculty of Health Sciences, University of Macau, Macao SAR, China

⁶Centre for Cognitive and Brain Sciences, University of Macau, Macao SAR, China

⁷Faculty of Health Sciences, University of Macau, Macao SAR, China

⁸School of Medicine, Hangzhou Normal University, Hangzhou, China

⁹Institute of sports medicine and health, Chengdu Sport University, Chengdu, China

Correspondence

Yu-Feng Zang, The Affiliated Hospital of Hangzhou Normal University, Hangzhou, 311121, Zhejiang, China.
 Email: zangyf@hznu.edu.cn

Jue Wang, Institute of Sports Medicine and Health, Chengdu Sport University, No. 2, Tiyuan Rd, Wuhou District, Chengdu, 610041, China.
 Email: juefirst@cdsu.edu.cn

Funding information

National Natural Science Foundation of China, Grant/Award Numbers: 81520108016, 82071537; Key Realm R&D Program of Guangdong Province, Grant/Award Number: 2019B030335001; Key Medical Discipline of Hangzhou, Grant/Award Number: 18JYXK046; The Cultivation Project of the Province-leveled Preponderant Characteristic Discipline of Hangzhou Normal University, Grant/Award Number: 20JYXK004

Abstract

Amplitude of low-frequency fluctuation (ALFF) has been widely used for localization of abnormal activity at the single-voxel level in resting-state fMRI (RS-fMRI) studies. However, previous ALFF studies were based on fast Fourier transform (FFT-ALFF). Our recent study found that ALFF based on wavelet transform (Wavelet-ALFF) showed better sensitivity and reproducibility than FFT-ALFF. The current study aimed to test the reliability and validity of Wavelet-ALFF, and apply Wavelet-ALFF to investigate the modulation effect of repetitive transcranial magnetic stimulation (rTMS). The reliability and validity were assessed on multicenter RS-fMRI datasets under eyes closed (EC) and eyes open (EO) conditions (248 healthy participants in total). We then detected the sensitivity of Wavelet-ALFF using a rTMS modulation dataset (24 healthy participants). For each dataset, Wavelet-ALFF based on five mother wavelets (i.e., db2, bior4.4, morl, meyr and sym3) and FFT-ALFF were calculated in the conventional band and five frequency sub-bands. The results showed that the reliability of both inter-scanner and intra-scanner was higher with Wavelet-ALFF than with FFT-ALFF across multiple frequency bands, especially db2-ALFF in the higher frequency band slow-2 (0.1992–0.25 Hz). In terms of validity, the multicenter ECEO datasets showed that the effect sizes of Wavelet-ALFF with all mother

This is an open access article under the terms of the [Creative Commons Attribution-NonCommercial](https://creativecommons.org/licenses/by-nc/4.0/) License, which permits use, distribution and reproduction in any medium, provided the original work is properly cited and is not used for commercial purposes.

© 2022 The Authors. *Human Brain Mapping* published by Wiley Periodicals LLC.

wavelets (especially for db2-ALFF) were larger than those of FFT-ALFF across multiple frequency bands. Furthermore, Wavelet-ALFF detected a larger modulation effect than FFT-ALFF. Collectively, Wavelet db2-ALFF showed the best reliability and validity, suggesting that db2-ALFF may offer a powerful metric for inspecting regional spontaneous brain activities in future studies.

KEYWORDS

amplitude of low-frequency fluctuation, fast Fourier transform, reliability, resting-state fMRI, validity, wavelet transform

1 | INTRODUCTION

Resting-state functional magnetic resonance imaging (RS-fMRI) is a powerful tool for investigating spontaneous neuronal activity. A growing body of neuroimaging studies has revealed brain network patterns by probing the relationships among separated brain regions at rest, which provides an overview of information communication within the brain networks and, furthermore, how these organizations are altered in neurological or psychiatric disorders (Harrison et al., 2008; van den Heuvel & Pol, 2010; Zuo & Xing, 2014). However, connections among brain regions are unable to reflect the local activity of a specific brain region, which plays a crucial role in the development of precision treatment for the clinic. The amplitude of low-frequency fluctuation (ALFF) is a widely used metric in local spontaneous brain activity at a single voxel (Zang et al., 2007) and has been used to precisely localize abnormal spontaneous brain activity in various diseases (Disner et al., 2018; Lencer et al., 2019; Li et al., 2022; Shang et al., 2018; Shang et al., 2019).

Conventionally, the fast Fourier transform (FFT) was conducted to calculate ALFF by converting a time series into the frequency domain by a set of sinusoidal functions. Compared to periodic sine function decomposition, the irregular shape of the mother wavelet (Goerke et al., 2005; Perraudin & Vandergheynst, 2017) is more suitable for modeling biological signals (Jallouli et al., 2021). Luo et al. (2020) first proposed Wavelet-ALFF in the analysis of RS-fMRI signals and reported that the sensitivity and reproducibility of Wavelet-ALFF were generally higher than those of FFT-ALFF. More specifically, ALFF based on the mother wavelet of Daubechies 2 (named db2-ALFF) was 1.54 times as sensitive as FFT-ALFF and 2.95 times more reproducible than FFT-ALFF in the higher frequency band (0.1992–0.25 Hz), which may be due to the similarity in the shape of the mother wavelet of db2 to the hemodynamic response function (HRF). However, the aforementioned results were obtained using four cohorts of attention-deficit/hyperactivity disorder (ADHD) RS-fMRI datasets. It should be noted that ADHD is a highly heterogeneous disorder, which may lead to ungeneralizable conclusions. The better reproducibility of Wavelet-ALFF needs to be demonstrated with more evidence.

Reliability and validity are always important considerations for the quality measurements of any metric (Zuo et al., 2019). To date, there has been no report on the test–retest reliability of Wavelet-ALFF. Therefore, our first aim was to investigate both the intra- and

inter-scanner reliability of Wavelet-ALFF. The validity of RS-fMRI metrics is not easily investigated in brain disorders due to the low reproducibility of RS-fMRI results across studies (Jia et al., 2021). However, the difference in ALFF between eyes closed (EC) and eyes open (EO) conditions has been well-documented in some brain regions by some RS-fMRI studies (Liu et al., 2013; Qian et al., 2019; Wei et al., 2018; Yuan et al., 2014). More importantly, the difference in these brain regions between EC and EO is very robust, and hence, could be taken as a reference for validity. Thus, the second aim of the current study was to test whether the Wavelet-ALFF has better validity than FFT-ALFF by employing nine RS-fMRI datasets containing EC and EO states in healthy participants.

To further test the superiority of Wavelet-ALFF over FFT-ALFF, we compared the sensitivity between Wavelet-ALFF and FFT-ALFF on a dataset of repetitive transcranial magnetic stimulation (rTMS) modulation study. rTMS has been widely used in the treatment of brain disorders (Lefaucheur et al., 2014; Lefaucheur et al., 2020; Rossi et al., 2021). Single-session rTMS modulation is a widely-accepted paradigm for studying causal effects in RS-fMRI studies (Bergmann et al., 2021; Wang et al., 2020). We recently found that a single-session of rTMS significantly modulated the FFT-ALFF in the dorsal anterior cingulate cortex (dACC) (Feng et al., 2021). We assumed that the effect size of rTMS modulation would likely be larger for Wavelet-ALFF than FFT-ALFF. Therefore, the current study investigated the improvement of Wavelet-ALFF in terms of reliability, validity, and sensitivity in detecting rTMS modulation effects.

2 | MATERIALS AND METHODS

2.1 | Data

2.1.1 | Multicenter ECEO datasets

Our study group collected a total of nine RS-fMRI datasets between 2007 and 2018, and the datasets were uploaded and made openly available at https://www.nitrc.org/projects/eceo_rsfmri_9/. The original dataset consisted of 260 participants, with 12 participants excluded due to incomplete information, bad spatial normalization, or excessive head motion (maximum head motion was larger than 2 mm or 2°). The remained data included scans from 248 subjects under EC

and EO conditions. The image acquisition parameters and demographic information were shown in Table 1 and Table S1, respectively. Two resting-state scans (EC and EO) were performed for each subject in a counterbalanced order for each dataset. Datasets 1–3 (hereafter named the reliability dataset) were collected from the same cohort of participants over three visits (V1, V2, and V3), where V1 and V2 (separated by 14 ± 1 days) were performed on a GE 3 T scanner and V3 was performed (230 ± 8 days after V2) on a Siemens 3 T scanner. Dataset 5 ($n = 19$; repetition time [TR] = 400 ms) is a subset of Dataset 4 ($n = 33$; TR = 2000 ms), that is, 19 of the 33 participants underwent an additional scan with a shorter TR. The ethics committee approved the collection of each dataset from the corresponding research center. All participants signed a written informed consent form before scanning. They were recruited by advertisement. All were right-handed and had no history of neurological or psychiatric illness. The participants were asked to lie on the scanner with their eyes naturally open (EO) or closed (EC), keep as still as possible, not fall asleep, and not think about anything in particular. Foam pads and straps were used to minimize head movement during scanning. After the RS-fMRI scan, the experimenter immediately talked to the participants and confirmed that none of them were asleep.

2.1.2 | Single-session rTMS modulation dataset

The RS-fMRI dataset of single-session rTMS stimulation in healthy adults ($N = 24$) was from a previous study (Feng et al., 2021). For the first visit, subjects underwent task-based fMRI and RS-fMRI to identify the effective region and stimulation targets for the following rTMS intervention. In our original article, Eriksen flanker task was used to define individual peak activation within the dorsal anterior cingulate cortex (dACC), which was chosen as the effective region. RS-fMRI was used to identify the stimulus target, that is, the voxel with the strongest functional connectivity to the effective region (i.e., the dACC). Subsequently, participants underwent rTMS intervention at four different targets (i.e., frontal, parietal, double, and sham targets) on four separate days (more than 1 week apart), and RS-fMRI scans were performed before and after each visit. For each visit, participants received 1800 pulses at 10 Hz frequency with 3-s trains (100% resting motor threshold) and 27-s inter-train interval. After individualized dACC-FC guided rTMS, FFT-ALFF was used to estimate the rTMS modulation effects. The finding (Feng et al., 2021) revealed that rTMS targeting right middle frontal gyrus (rMFG) modulates FFT-ALFF in the dACC. Furthermore, functional connectivity (FC) strength before rTMS (i.e., pre-rTMS FC) predicts FFT-ALFF changes in the dACC. Here, we examined whether Wavelet-ALFF would show higher sensitivity over FFT-ALFF in detecting the modulation effect of rTMS. Also, sham stimulation session was included for analysis for comparison. This rTMS study was approved by the ethics committee of the Center for Cognitive and Brain Disorders, Hangzhou Normal University. All subjects signed informed consent forms. The details of the rTMS experimental design were described in prior study (Feng et al., 2021). Detailed information on all datasets was shown in Figure 1 and Table 1.

2.2 | Data preprocessing

All RS-fMRI data were preprocessed using DPABI (Yan & Zang, 2010) based on MATLAB (<https://www.mathworks.com/>) and SPM12 (<https://www.fil.ion.ucl.ac.uk/spm/>) with the following procedures: removing the first 20 s of the brain volumes, slice time correction, motion correction, spatial normalization via nonlinear registration to an EPI template with a resampling resolution of $3 \times 3 \times 3$ mm, and spatial smoothing with a Gaussian kernel of 6 mm in three directions. The Friston 24-parameter model (Friston et al., 1996) was used to reduce the potential effect of head motion, and the averaged time courses of cerebrospinal fluid (CSF) and white matter were considered nuisance variables and were regressed out from each voxel's time series using a multiple regression model.

2.3 | ALFF calculation

FFT-ALFF was calculated using DPABI toolkit. The power spectrum was acquired by converting the preprocessed time series of each voxel to the frequency domain using FFT. The averaged square root was extracted from the power spectrum of each voxel across a given frequency band (named FFT-ALFF). For normalization purposes, the FFT-ALFF of each voxel was divided by the global mean FFT-ALFF.

Wavelet-ALFF was computed using the RESTplus toolkit. Continuous wavelet transform (CWT) is a method for decomposing a single time series into a time-frequency domain by continuously convolving the time series $x(t)$ with dilated and translated versions of a wavelet function ψ_0 (Luo et al., 2020; Sifuzzaman et al., 2009; Torrence & Compo, 1998). The function of CWT is defined as follows:

$$CWT(k, s) = \frac{1}{\sqrt{s}} \int_{-\infty}^{+\infty} x(t) \cdot \psi_0 \left(\frac{t-k}{s} \right) dt \quad (1)$$

where $x(t)$ is the time series and $s \in R^+$ and k are wavelet scales (64 frequency bins were selected from 0 to 0.25 Hz at an interval of 0.0039 Hz for this study) and localized time index, respectively.

The wavelet coefficients at each scale and each time point were obtained following the above steps, and Wavelet-ALFF is the average of the wavelet coefficients in a given frequency band. To reduce the effects of between-subject variability, Wavelet-ALFF was further standardized by dividing by the global mean Wavelet-ALFF.

As did in a previous study (Luo et al., 2020), 5 mother wavelets were selected, namely, Biorthogonal 4.4 (bior4.4) (Sweldens, 1996; Wang et al., 2016), Daubechies 2 (db2) (Desco et al., 2001; Dinov et al., 2005; Lina & Mayrand, 1995), Morlet (morl) (Chang & Glover, 2010; Yaesoubi et al., 2015; Yuan et al., 2010; Zotev et al., 2014), Meyer (meyr) (Behjat et al., 2015) and Symlets 3 (sym3) (Desco et al., 2001; Khullar et al., 2011). The features of different mother wavelets are shown in Figure S1.

Consistent with previous frequency sub-bands ALFF studies (Zhang et al., 2015; Zuo, Di Martino, et al., 2010a), FFT-ALFF and Wavelet-ALFF were calculated in the conventional band (0.0117–0.0781 Hz) and five sub-bands: slow-6 (0–0.0117 Hz), slow-5

TABLE 1 Scanning parameters of the multicenter RS-fMRI datasets under eyes closed (EC) and eyes open (EO) conditions and of the rTMS dataset.

	Number of participants	Center	Model	Manufacture	TR (s)	TE (ms)	Flip angle (°)	Matrix size	File of view (mm ³)	Voxel size (mm ³)	Gap (mm)	Slice thickness (mm)	Slice number	Total scan time (min)	Slice acquisition order
Dataset 1-2	21	HNU	Discovery MR-750	GE	2	30	90	64 × 64	220 × 220	3.44 × 3.44 × 3.2	0	3.2	43	8	Interleaved, ascending
Dataset 3	21	ZJU	Prisma	Siemens	2	30	90	64 × 64	220 × 220	3.44 × 3.44 × 3.4	0	3.4	43	8	Interleaved, ascending
Dataset 4	29	HNU	Discovery MR-750	GE	2	30	60	64 × 64	220 × 220	3.44 × 3.44 × 3.2	0	3.2	43	8	Interleaved, ascending
Dataset 5	41	HNU	Discovery MR-750	GE	0.4	15	30	64 × 64	240 × 240	3.75 × 3.75 × 7	1	6	43	8	Interleaved, ascending
Dataset 6	43	BNU	MAGNETOM TrioTim	Siemens	2	30	90	64 × 64	200 × 200	3.1 × 3.1 × 3.5	0	3.5	33	8	Interleaved, ascending
Dataset 7	33	HNU	Discovery MR-750	GE	2	30	90	64 × 64	220 × 220	3.44 × 3.44 × 3.2	0	3.2	43	8	Interleaved, ascending
Dataset 8	20	BNU	MAGNETOM TrioTim	Siemens	2	30	90	64 × 64	200 × 200	3.125 × 3.125 × 3.6	0	3.6	33	8	Interleaved, ascending
Dataset 9	17	HNU	Discovery MR-750	GE	0.4	15	30	64 × 64	240 × 240	3.75 × 3.75 × 7	6	1	13	8	Interleaved, ascending
rTMS dataset	24	HNU	Discovery MR-750	GE	2	30	90	64 × 64	220 × 220	3.44 × 3.44 × 3.2	0	3.2	43	8	Interleaved, ascending

Note: The multicenter ECEO datasets were obtained from Hangzhou Normal University (HNU), Zhejiang University (ZJU) and Beijing Normal University (BNU). Dataset 1–3 are the reliability datasets. Dataset 5 is a subset of dataset 4, in which subjects underwent two sets of RS-fMRI scans under EC and EO conditions with different acquisition parameters. Abbreviations: TR, time of repetition; TE, time of echo.

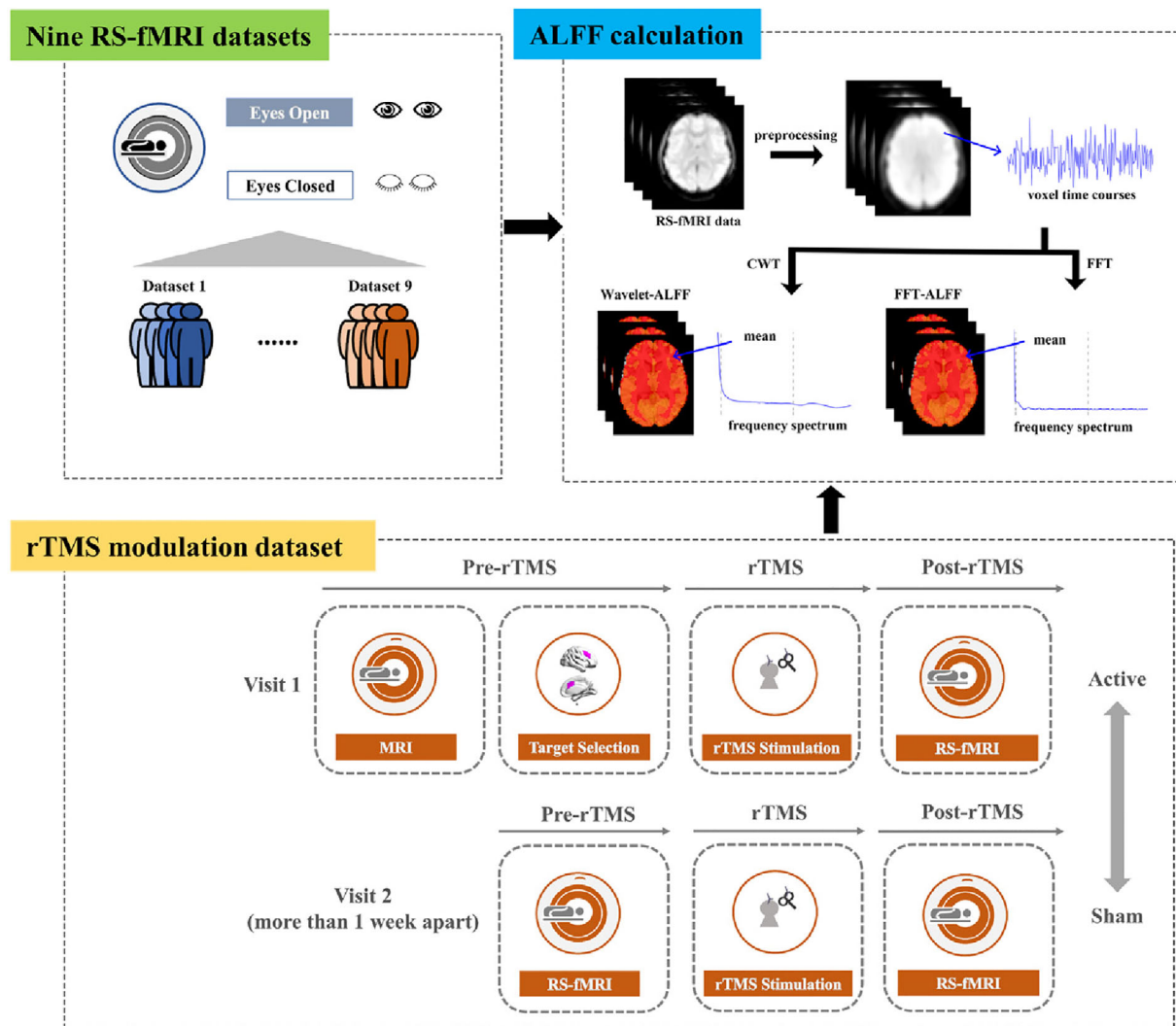


FIGURE 1 The flowchart of multicenter ECEO RS-fMRI datasets and rTMS dataset information, ALFF calculation. ALFF: Amplitude of low-frequency fluctuation.

(0.0117–0.0273 Hz), slow-4 (0.0273–0.0742 Hz), slow-3 (0.0742–0.1992 Hz), and slow-2 (0.1992–0.25 Hz). The flowchart of ALFF calculation was shown in Figure 1.

2.4 | Statistical analysis

2.4.1 | Test–retest reliability analyses for the reliability dataset

The reliability dataset was used to inspect the intra-scanner (i.e., V1 vs. V2) and inter-scanner (i.e., V1 vs. V3, V2 vs. V3) reliability of FFT- and Wavelet-ALFF using the intraclass correlation (ICC) (Shrout & Fleiss, 1979) of each frequency band and each resting state (EC and EO) as follows:

$$ICC = \frac{MS_b - MS_w}{MS_b + (k - 1)MS_w} (2)$$

where MS_b is the between-subject variance, MS_w is the within-subject variance, k is the number of sessions, and $k = 2$ for the ICC calculation.

2.4.2 | Validity analyses for multicenter EC-EO datasets: Mega-analyses with paired sample t test and two-sample t test

The validity analyses were performed on multicenter RS-fMRI datasets under EC and EO conditions. An empirical Bayesian estimation method named Combat (Beer et al., 2020) was used to remove the potential scanner variability, in which the head movement parameters (i.e., mean framewise displacement) were used as covariates, and their effects were regressed. Then, all data were entered into mega-analyses with both the paired t test and the two-sample t test as follows.

Paired t tests were performed between EC and EO on each measure at each frequency band. Voxels above the corrected threshold

(Gaussian random field theory correction [GRF correction], single voxel $p < .001$, cluster level $p < .05$) were taken as showing a significant difference in ALFF between EC and EO. Additionally, we performed two-sample t tests since the between-group comparison is much more prevalent in clinical studies, and between-group designs are more challenging for reproducibility due to intersubject variability. For grouping, half of the participants were selected as group 1 and the rest were selected as group 2. The age, sex, and scanning order of EC and EO were well matched ($p > .5$, Table S2) between the two groups in each dataset. Two-sample t tests were performed between EC in group 1 and EO in group 2 at each frequency band for FFT-ALFF and Wavelet-ALFF. The threshold of between-group comparisons was identical to that of within-group comparisons.

To compare the validity of Wavelet-ALFF and FFT-ALFF metrics, we compared the cumulative distributions of effect sizes for the differences between EC and EO detected by these measures.

2.4.3 | Application of Wavelet-ALFF on the modulation effect of rTMS

The single-session rTMS modulation dataset was used to test the sensitivity of Wavelet-ALFF and FFT-ALFF in measuring changes in local

brain activity. A spherical region of interest (ROI) (radius = 4 mm) was centered at the individualized dACC location. Paired t tests were performed on the mean Wavelet-ALFF and FFT-ALFF values within the dACC-ROI to compare between pre- and post-rTMS.

Moreover, FC between the rMFG-ROI (centered at the stimulation target with a 4 mm radius) and the dACC-ROI was calculated (Feng et al., 2021b). We performed Pearson's correlation analyses between the strength of FC and the mean Wavelet-ALFF and FFT-ALFF changes (post-rTMS minus pre-rTMS) in the dACC-ROI to investigate whether the strength of FC could predict the modulation effect by rTMS in multiple frequency sub-bands.

3 | RESULTS

3.1 | Intra- and inter-scanner reliability

The reliability results are generally summarized as follows:

1. ICC values were generally the highest for db2-ALFF, while the ICC for FFT-ALFF was the lowest for both intra- and inter-scanner observations and in both EC and EO resting states in all frequency bands (Figure 2b,c; Figure S2-S7; Table S3). Especially with the

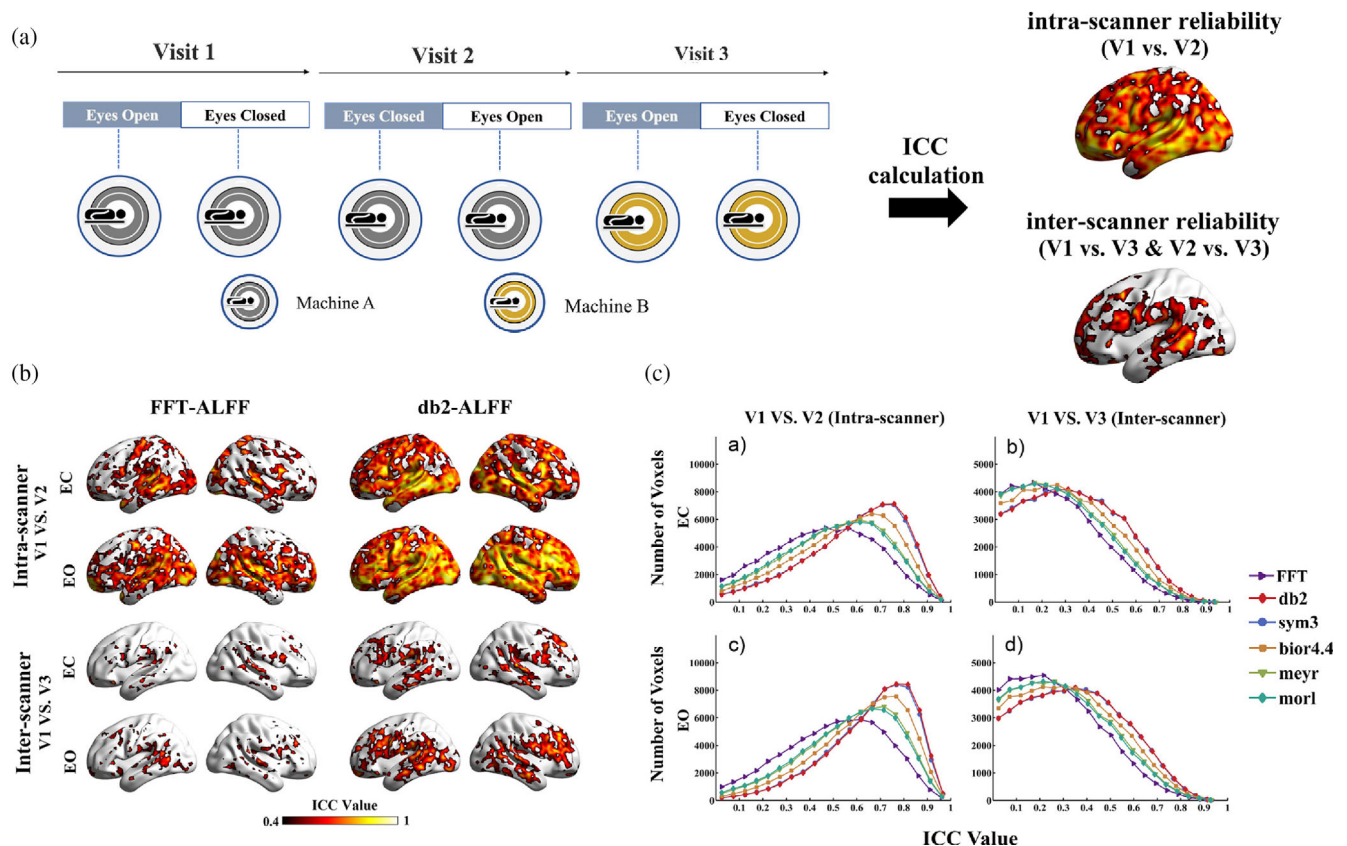


FIGURE 2 The reliability of wavelet-ALFF was higher than that of FFT-ALFF. (a) Flowchart of the reliability dataset information and ICC calculation. (b) the intra- and inter-scanner reliability of FFT-ALFF, db2-ALFF of eyes open (EO) and eyes closed (EC) in the higher frequency band slow-2 (0.1992–0.25 Hz). (c) the comparison of the reliability histogram among FFT-, db2-, sym3-, bior4.4-, meyr-, morl-ALFF of EO and EC in slow-2 (0.1992–0.25 Hz). If the distribution curve of the ICC value tends to be plotted on the right side of the graph, the reliability of the metric is better. Intra-scanner reliability (a, c); Inter-scanner reliability (b, d). ICC, intra-class correlation; V, visit; ALFF, amplitude of low-frequency fluctuation; FFT, fast Fourier transform; db2, Daubechies 2; sym3, Symlets 3; bior4.4, biorthogonal 4.4; meyr, Meyer; morl, Morlet.

higher frequency band slow-2 (0.1992–0.25 Hz), the intra- and inter-scanner reliability of db2-ALFF was much higher than that of FFT-ALFF (Figure 2b,c).

- The ICCs of EC and EO were approximately the same across all frequency sub-bands (Figure 2b; Figure S2, S8–S13).

3.2 | Differences between Wavelet-ALFF and FFT-ALFF in detecting the difference between EC and EO

The spatial pattern of the difference between EC and EO conditions was highly consistent with that in previous studies (Yang et al., 2007; Yuan et al., 2014; Zhao et al., 2018; Zou et al., 2015a; Zou et al., 2015b) on both Wavelet-ALFF (five mother wavelets: db2, bior4.4, meyr, morl, and sym3) and FFT-ALFF. EC had higher ALFF than EO in the bilateral sensorimotor cortex and supplementary motor area (SMA), while EC had lower ALFF than EO in the bilateral frontal gyrus and middle occipital gyrus (MOG) (Figure S14 and S15).

Regarding the comparison between Wavelet-ALFF and FFT-ALFF, effect sizes were almost the largest for db2-ALFF and approximately the smallest for FFT-ALFF in all frequency bands in all brain regions, showing a significant difference between EC and EO (Figure 3; Figure S16 and S17). The larger effect size of db2-ALFF than FFT-ALFF was observed across all frequency sub-bands and the conventional band (Figure 3a). This larger effect size was the most prominent in the slow-2 frequency band for both between-group and within-group comparisons (Figure 3b).

3.3 | Modulation effect of rTMS: Wavelet-ALFF versus FFT-ALFF

We first compared the modulation effect of rTMS measured by FFT-ALFF in the conventional band, and the results were the same as those of our previous study (Feng et al., 2021b). More importantly, FFT-ALFF in all frequency sub-bands were calculated, and the Wavelet-ALFF of five mother wavelets were also used to measure the

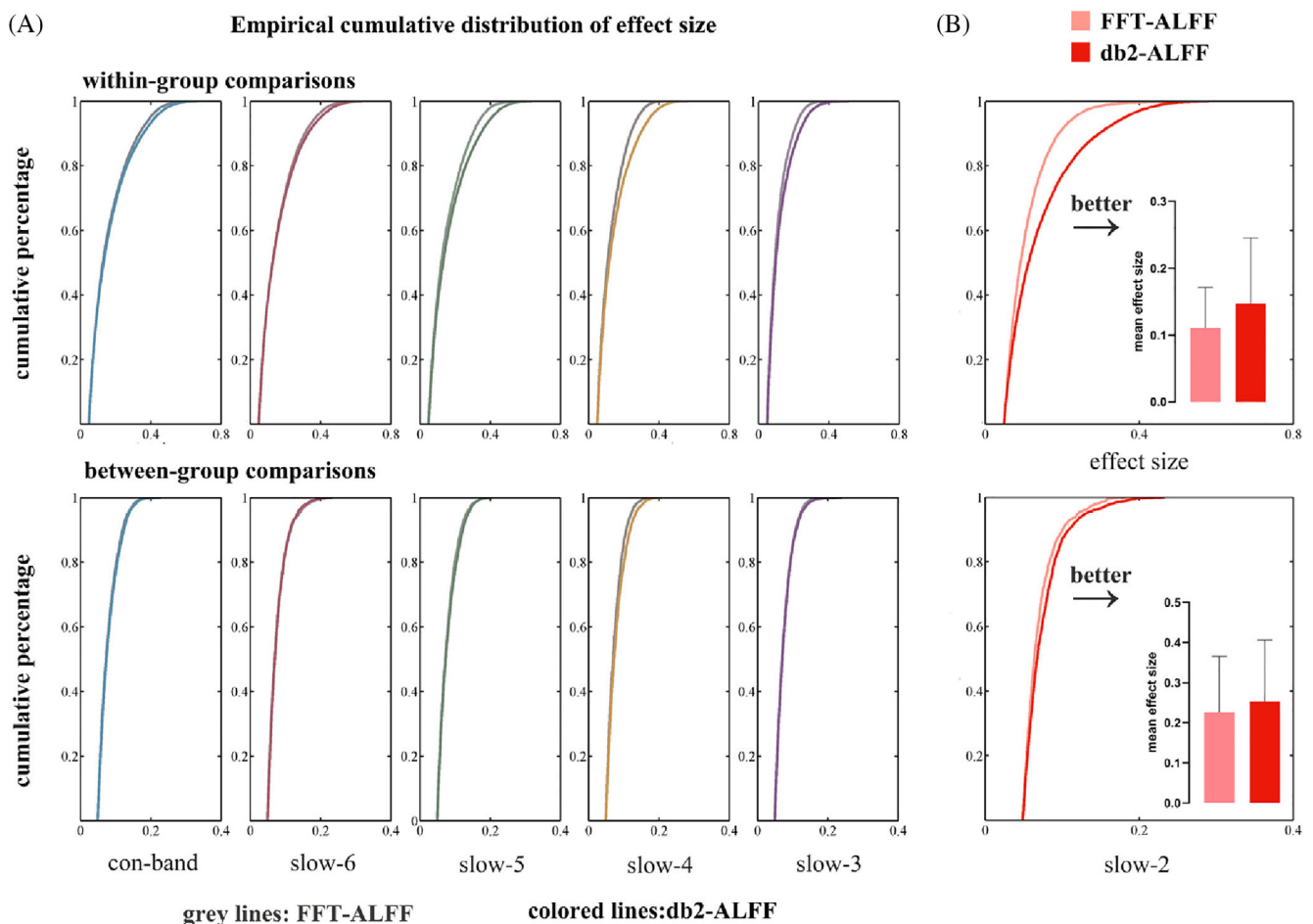


FIGURE 3 The differences between EC and EO calculated from db2-ALFF showed larger effect sizes than FFT-ALFF. Under the conditions of comparisons within groups (upper) and comparisons between groups (bottom), (a) the empirical distribution and bar plots of mean effect size with error bars (standard deviation) for detecting db2-ALFF and FFT-ALFF differences between EC and EO in the slow-2 frequency band (0.1992–0.25 Hz); (b) the empirical cumulative distribution of effect sizes for each frequency band in within-group comparisons (upper) and between-group comparisons (bottom). The distribution of effect size from FFT-ALFF was shown in gray, while colored lines represented effect sizes from db2-ALFF. GRF corrected, voxel $p < .001$, cluster $p < .05$; Cohen's f^2 was the measure for calculating effect sizes in the current study.

modulation effect of rTMS in all frequency sub-bands and the conventional band. Both Wavelet-ALFF and FFT-ALFF revealed significant differences between pre- and post-TMS, and the effect sizes of Wavelet-ALFF were larger than that of FFT-ALFF in all cases (five mother wavelets and six frequency bands) (Figure 4, Table S4-S6). This larger effect size was more prominent for db2-ALFF and sym3-ALFF (Figure 4 and Figure S18). In the conventional band and all frequency sub-bands, paired *t* tests showed that sham rTMS stimulation did not significantly modulated Wavelet-ALFF and FFT-ALFF in the dACC (Table S4-S9).

As did in our previous study (Feng et al., 2021), we examined the correlation between the pre-rTMS FC and FFT-ALFF changes in the dACC in the conventional band (0.0117–0.0781 Hz) and replicated our previous result (Figure 5d). Furthermore, correlation analyses were performed between the pre-rTMS FC and the changes in both Wavelet-ALFF and FFT-ALFF in the dACC in all frequency sub-bands. The results showed that the correlation values between pre-rTMS FC and Wavelet-ALFF changes were similar to those between pre-rTMS FC and FFT-ALFF changes (Figure 5). Moreover, no significant correlation between the pre-rTMS of the sham condition and the changes in local brain activity (i.e., Wavelet-ALFF and FFT-ALFF) was found (Figure S19). In addition, similar results were obtained under controlling the distance between the stimulation target and effective region (Figure S20).

4 | DISCUSSION

The current study systematically investigated the intra- and inter-scanner reliability and validity of Wavelet-ALFF across multiple frequency bands. We found that the intra- and inter-scanner reliability of Wavelet-ALFF was generally higher than that of FFT-ALFF, especially db2-ALFF in the higher frequency band slow-2 (0.1992–0.25 Hz). When comparing EC and EO conditions from 9 RS-fMRI datasets, both within-group and between-group comparisons revealed larger effect sizes for Wavelet-ALFF than FFT-ALFF. This was especially true with slow-2 (0.1992–0.25 Hz), in which db2-ALFF exhibited much more robust differences between EC and EO conditions than FFT-ALFF. Moreover, we applied Wavelet-ALFF to the rTMS modulation dataset and found that Wavelet-ALFF detected larger modulation effect than FFT-ALFF.

4.1 | Higher intra- and inter-scanner reliability of Wavelet-ALFF

Reliability is one of the most critical concerns for any metric. ALFF has been widely used to localize aberrant functions at the level of single voxels (Fu et al., 2018; Turner et al., 2013; Zang et al., 2007; Zang et al., 2015; Zheng et al., 2021). All of these studies were based on

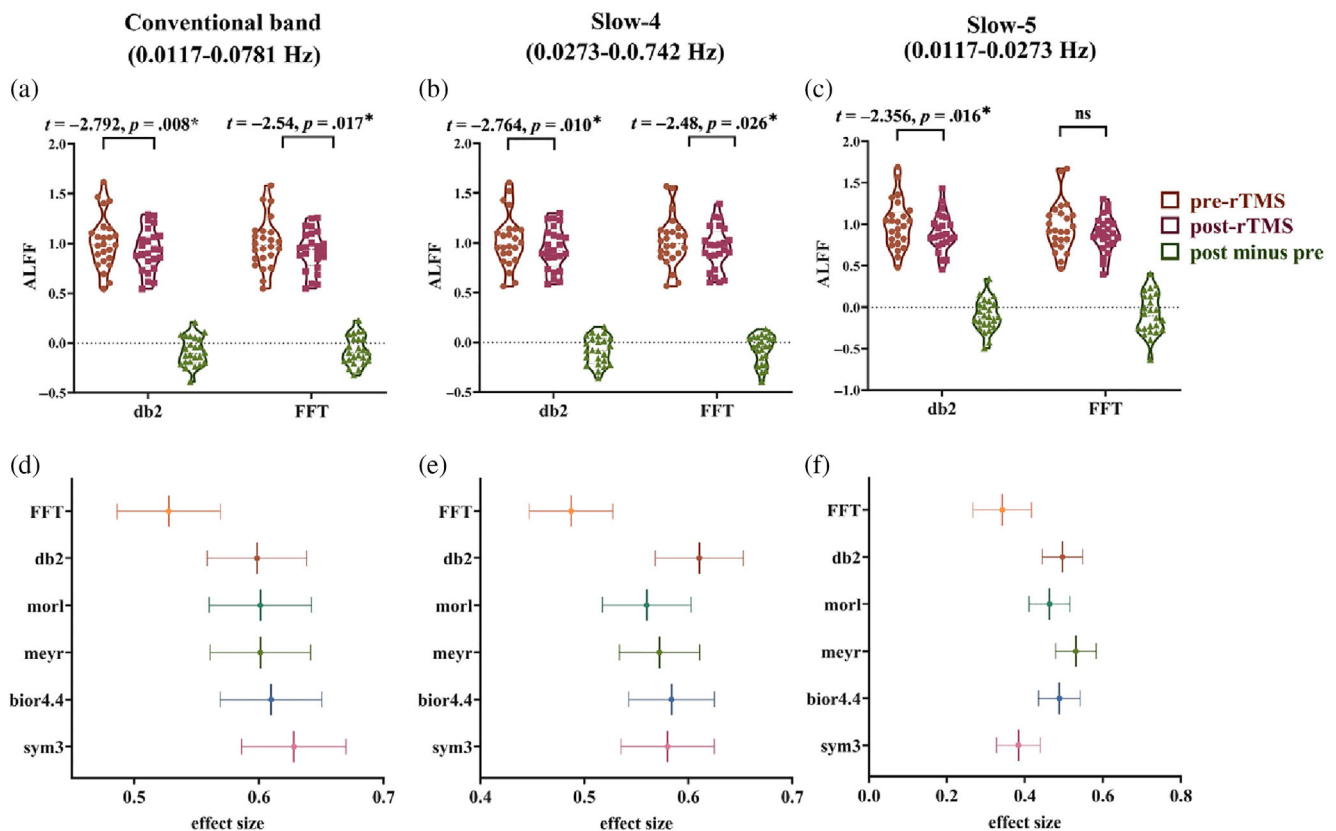


FIGURE 4 The db2-ALFF and FFT-ALFF measured rTMS-induced local activity changes in the dACC. Paired *t* tests (post-rTMS vs. pre-rTMS) showed significantly decreased db2-ALFF and FFT-ALFF in the dACC under the condition of real stimulation in conventional band (a) and slow-4 (b), in which the effect sizes of wavelet-ALFF were higher than that of FFT-ALFF (D, E). In slow-5 (0.0117–0.0273 Hz), paired *t* tests showed a significantly decreased db2-ALFF while a decreased trend of FFT-ALFF (C, F). **p* < .05.

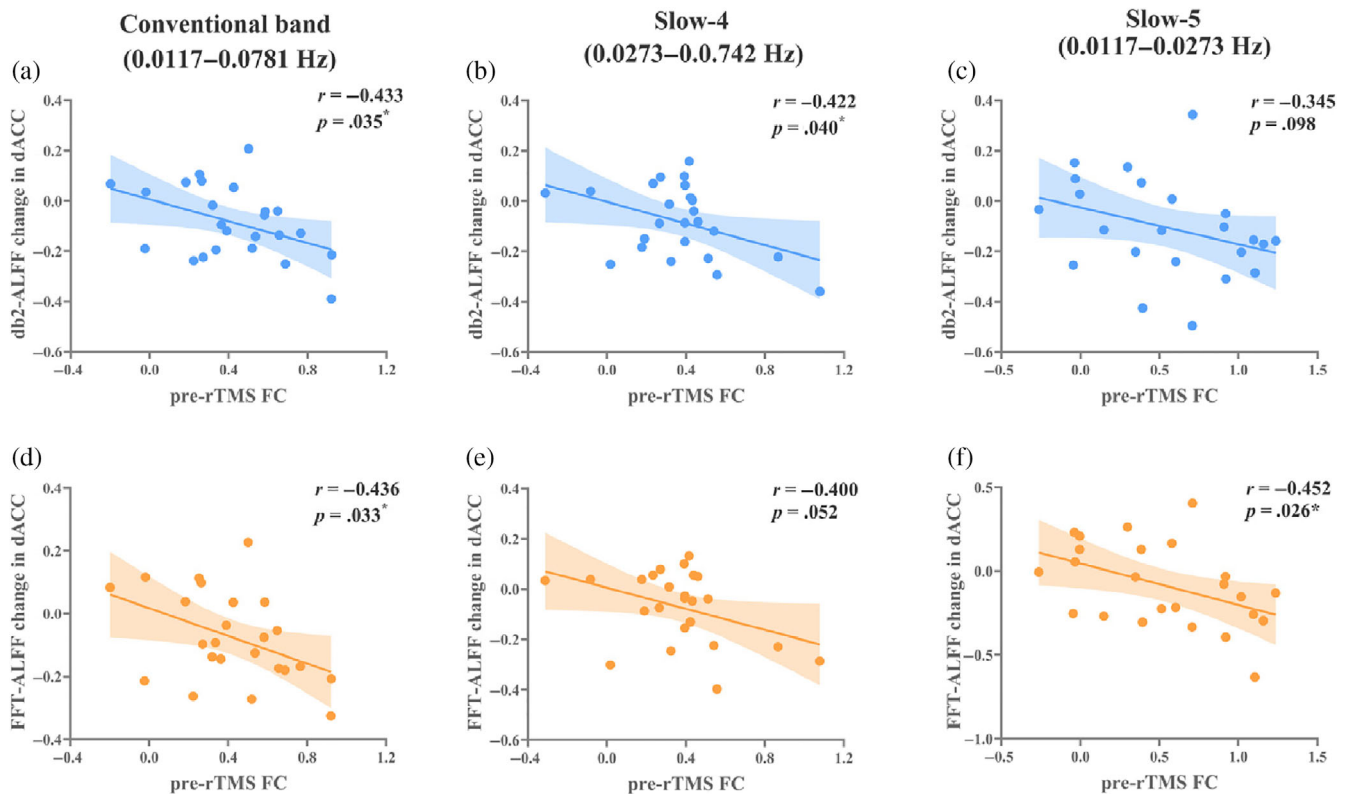


FIGURE 5 Correlations between pre-rTMS FC and the db2-ALFF (upper in blue) and FFT-ALFF (lower in orange) changes in the dACC. In the conventional band, pre-rTMS FC was significantly correlated with the db2-ALFF changes (a) and FFT-ALFF changes (D) in the dACC. For the sub-bands, while the correlation pattern was similar for db2-ALFF (B, C) and FFT-ALFF (E, F), they showed slightly different correlation values. * $p < .05$.

FFT-ALFF; however, our recent study found that Wavelet-ALFF had better sensitivity and reproducibility (Luo et al., 2020). The current study first investigated the reliability of Wavelet-ALFF for application purposes. Although studies have shown that FFT-ALFF possesses a high test-retest reliability (Zuo, Kelly, et al., 2010b; Zuo & Xing, 2014), we found that both the intra- and inter-scanner reliability of Wavelet-ALFF was generally higher than that of FFT-ALFF in EC and EO states across multiple frequency bands. Of note, the intra- and inter-scanner reliability of db2-ALFF was much higher than that of FFT-ALFF, especially in the higher frequency band slow-2 (0.1992–0.25 Hz). Therefore, db2-ALFF is a reliable measurement to explore brain function and has possible implications in its potential for probing developmental and pathological processes (Bennett & Miller, 2010; Hodkinson et al., 2013; Zuo, Kelly, et al., 2010b).

4.2 | Higher validity of Wavelet-ALFF

A good metric should have both high reliability and validity (Vollmar et al., 2010). In the comparison of a variety of methods for reliability measurement, validity is usually assessed based on a previously established, definitive reference standard (or a “gold” standard) (Wilson et al., 2017). Given the high heterogeneity in RS-fMRI studies for detecting the difference between patients and healthy controls, it is

challenging to develop a metric with high validity for RS-fMRI. However, the difference between EC and EO states in healthy participants has been revealed very consistently across RS-fMRI studies, and this difference is mainly observed in the bilateral sensorimotor cortex, SMA, and MOG (Agcaoglu et al., 2019; Agcaoglu et al., 2020; Y. X. Feng et al., 2021; Liu et al., 2013; Wei et al., 2018; Yang et al., 2007; Yuan et al., 2014; Yuan et al., 2018; Zhao et al., 2018). The current study pooled multicenter datasets including EC and EO conditions, and both within-subject and between-subject comparisons demonstrated that the effect size with Wavelet-ALFF for most wavelet bases was larger than that of FFT-ALFF across multiple frequency bands, especially for db2-ALFF in the higher frequency band slow-2 (0.1992–0.25 Hz). Hence, we can therefore conclude that the validity of Wavelet-ALFF is higher than that of FFT-ALFF.

Moreover, we were interested in whether Wavelet-ALFF could detect larger effect sizes in the rTMS modulation data. When Wavelet-ALFF and FFT-ALFF were used to detect rTMS-induced changes in individualized dACC location, both measures detected the modulation effect of rTMS in the same direction, although FFT-ALFF had a smaller effect size. In other words, the use of Wavelet-ALFF increased the statistical significance (i.e., larger effect sizes) of the differences between pre-rTMS and post-rTMS. Based on these findings, we recommend applying Wavelet-ALFF to detect changes in local brain activity in RS-fMRI studies.

4.3 | Shape of db2 and the hemodynamic response function (HRF)

Wavelet-ALFF is superior to FFT-ALFF in reliability and validity, in which db2-ALFF is the most robust metric for detecting spontaneous local activity. Previous studies have shown that the wavelet transform is highly sensitive to relatively large oscillatory activity (Dinov et al., 2005; van Vugt et al., 2007; Zhang et al., 2016). The brain regions involved in visuospatial processing generated higher oscillatory activity during the EO state than the EC state (Boros et al., 2016), which resulted in Wavelet-ALFF revealing more differences in the MOG between the EC and EO conditions. Furthermore, the critical factor in modeling biological structures and patterns is selecting a suitable basis function (Chang & Glover, 2010; Khullar et al., 2011; Lio, 2003). Among the five mother wavelets, the shape of db2 is quite similar to that of the HRF (Figure 6); hence, wavelet functions appear to be a more accurate way to model the HRF (Lindquist & Wager, 2007). Lewis et al. (2016) found that the shape of the HRF depended on the duration of neural activity, in which a narrower HRF produced larger responses in the higher frequency band. Combining the previous suggestions and our results, we hypothesize that the db2 mother wavelet is more suitable for modeling HRF at higher frequency activities.

4.4 | Physiological significance of higher frequency oscillations and db2-ALFF

The db2-ALFF data showed the most robust reliability and validity, especially in the higher frequency band slow-2 (0.1992–0.25 Hz). Generally, higher frequency oscillations of RS-fMRI signals have long been considered primarily physiological noise. However, an electrophysiology study demonstrated that there was a link between electrical activity in electroencephalography (EEG) and the higher frequency

(>0.1 Hz) component of the fMRI signal, in which the faster dynamics of the fMRI response were accompanied by continuous and rapid changes in neural activity (Lewis et al., 2016). In line with a previous study (Yuan et al., 2014), we also found that both the higher and lower frequency bands showed different oscillations between EC and EO states. In addition to the higher frequency functional significance based on physiological evidence (Boubela et al., 2013; Chen & Glover, 2015; DeRamus et al., 2021), the higher frequency amplitude in the fMRI signal may provide novel biomarkers for use in the clinic (Malinen et al., 2010; Otti et al., 2013; Wang et al., 2015; Wee et al., 2012). We found that in both the higher and lower frequency bands, the differences between EC and EO conditions were always present in brain regions backed by solid and valid evidence (Agcaoglu et al., 2019; Yuan et al., 2014; Zou et al., 2015b). Among the metrics, db2-ALFF was the most sensitive in the slow-2 sub-band in these brain regions. Therefore, we suggest that db2-ALFF can be used in resting-state studies to analyze the higher frequency signals.

As for the definition of lower and higher frequency in RS-fMRI studies, there has been no consensus on how many frequency bands should be divided, e.g., three bands (Malinen et al., 2010), six bands (Otti et al., 2013), and five bands (Zuo, Di Martino, et al., 2010a) for TR = 2 s; but more complicated for short TR (Yuan et al., 2014). Most ALFF sub-frequency studies have followed Zuo, Di Martino, et al. (2010a), that is, five bands. These ALFF studies used “ALFF” to represent all sub-bands while use “lower” and “higher” to differentiate the sub-bands. It might be helpful to rename the different frequency bands in the future RS-fMRI studies.

4.5 | Limitations

A few limitations of the current study should be addressed. First, the inter-scanner interval was too long (approximately half a year), and the scanning order was not counterbalanced. Second, wavelet

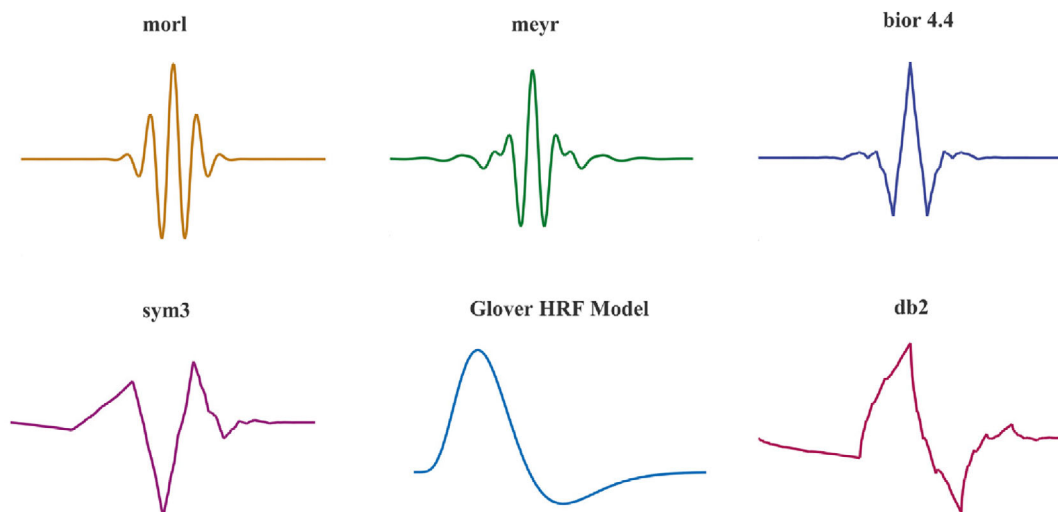


FIGURE 6 Time course of the simulated HRF from Glover 1999 and wavelet function of 5 mother wavelets (i.e., db2, bior 4.4, meyr, morl, and sym3).

transformation is an efficient time-frequency transformation. We did not use the temporal domain information from the wavelet transformation to compare with FFT-ALFF. Hence, further studies need to solve how to better utilize the temporal information. Third, only healthy individuals were used in this analysis, we need to further explore whether the advantages of Wavelet-ALFF still exist under different scanning parameters, different populations, and different brain diseases.

5 | CONCLUSION

To conclude, this study provides evidence of the superiority of Wavelet-ALFF (especially db2-ALFF) over FFT-ALFF in improving reliability and validity and increasing statistical significance. Therefore, we recommend db2-ALFF for the analysis of RS-fMRI signals in both low- and high-frequency bands.

ACKNOWLEDGMENTS

The study was supported by NSFC (82071537, 81520108016), Key Realm R&D Program of Guangdong Province (2019B030335001), Key Medical Discipline of Hangzhou, and The Cultivation Project of the Province-leveled Preponderant Characteristic Discipline of Hangzhou Normal University (18JYXK046, 20JYXK004).

CONFLICT OF INTEREST

The authors have no conflicts of interest to declare.

DATA AVAILABILITY STATEMENT

The multicenter RS-fMRI datasets under EC and EO conditions were uploaded to the open-access NITRC (https://www.nitrc.org/projects/eceo_rsfmri_9/). The datasets of between-group design strictly matched for gender, age and scanning order were also shared. The rTMS modulation data that support the findings of this study are available from the corresponding author upon reasonable request.

ORCID

Zi-Jian Feng  <https://orcid.org/0000-0002-7228-3383>

Jue Wang  <https://orcid.org/0000-0003-4790-4827>

Yu-Feng Zang  <https://orcid.org/0000-0003-1833-8010>

REFERENCE

- Agcaoglu, O., Wilson, T. W., Wang, Y. P., Stephen, J., & Calhoun, V. D. (2019). Resting state connectivity differences in eyes open versus eyes closed conditions. *Human Brain Mapping, 40*(8), 2488–2498. <https://doi.org/10.1002/hbm.24539>
- Agcaoglu, O., Wilson, T. W., Wang, Y. P., Stephen, J. M., & Calhoun, V. D. (2020). Dynamic resting-state connectivity differences in eyes open versus eyes closed conditions. *Brain Connectivity, 10*(9), 504–519. <https://doi.org/10.1089/brain.2020.0768>
- Bennett, C. M., & Miller, M. B. (2010). How reliable are the results from functional magnetic resonance imaging? *Year in Cognitive Neuroscience, 2010*(1191), 133–155. <https://doi.org/10.1111/j.1749-6632.2010.05446.x>
- Bergmann, T. O., Varatheeswaran, R., Hanlon, C. A., Madsen, K. H., Thielscher, A., & Siebner, H. R. (2021). Concurrent TMS-fMRI for causal network perturbation and proof of target engagement. *NeuroImage, 237*, 118093. <https://doi.org/10.1016/j.neuroimage.2021.118093>
- Boros, M., Anton, J. L., Pech-Georgel, C., Grainger, J., Szwed, M., & Ziegler, J. C. (2016). Orthographic processing deficits in developmental dyslexia: Beyond the ventral visual stream. *NeuroImage, 128*, 316–327. <https://doi.org/10.1016/j.neuroimage.2016.01.014>
- Boubela, R. N., Kalcher, K., Huf, W., Kronnerwetter, C., Filzmoser, P., & Moser, E. (2013). Beyond noise: Using temporal ICA to extract meaningful information from high-frequency fMRI signal fluctuations during rest. *Frontiers in Human Neuroscience, 7*, 168. <https://doi.org/10.3389/fnhum.2013.00168>
- Chang, C., & Glover, G. H. (2010). Time-frequency dynamics of resting-state brain connectivity measured with fMRI. *NeuroImage, 50*(1), 81–98. <https://doi.org/10.1016/j.neuroimage.2009.12.011>
- Chen, J. E., & Glover, G. H. (2015). BOLD fractional contribution to resting-state functional connectivity above 0.1 Hz. *NeuroImage, 107*, 207–218. <https://doi.org/10.1016/j.neuroimage.2014.12.012>
- DeRamus, T., Faghiri, A., Iraj, A., Agcaoglu, O., Vergara, V., Fu, Z. N., Silva, R., Gazula, H., Stephen, J., Wilson, T. W., Wang, Y. P., & Calhoun, V. (2021). Modular and state-relevant functional network connectivity in high-frequency eyes open vs eyes closed resting fMRI data. *Journal of Neuroscience Methods, 358*, 109202. <https://doi.org/10.1016/j.jneumeth.2021.109202>
- Dinov, I. D., Boscardin, J. W., Mega, M. S., Sowell, E. L., & Toga, A. W. (2005). A wavelet-based statistical analysis of fMRI data. *Neuroinformatics, 3*(4), 319–342. <https://doi.org/10.1385/Nl:3:4:319>
- Disner, S. G., Marquardt, C. A., Mueller, B. A., Burton, P. C., & Sponheim, S. R. (2018). Spontaneous neural activity differences in posttraumatic stress disorder: A quantitative resting-state meta-analysis and fMRI validation. *Human Brain Mapping, 39*(2), 837–850. <https://doi.org/10.1002/hbm.23886>
- Feng, Y. X., Li, R. Y., Wei, W., Feng, Z. J., Sun, Y. K., Sun, H. Y., Tang, Y. Y., Zang, Y. F., & Yao, K. (2021a). The acts of opening and closing the eyes are of importance for congenital blindness: Evidence from resting-state fMRI. *NeuroImage, 233*, 117966. <https://doi.org/10.1016/j.neuroimage.2021.117966>
- Feng, Z. J., Deng, X. P., Zhao, N., Jin, J., Yue, J., Hu, Y. S., Jing, Y., Wang, H. X., Knosche, T. R., Zang, Y. F., & Wang, J. (2021b). Resting-state fMRI functional connectivity strength predicts local activity change in the dorsal cingulate cortex: A multi-target focused rTMS study. *Cerebral Cortex, 32*, 2773–2784. <https://doi.org/10.1093/cercor/bhab380>
- Fu, Z., Tu, Y., Di, X., Du, Y., Pearlson, G. D., Turner, J. A., Biswal, B. B., Zhang, Z., & Calhoun, V. D. (2018). Characterizing dynamic amplitude of low-frequency fluctuation and its relationship with dynamic functional connectivity: An application to schizophrenia. *NeuroImage, 180* (Pt B), 619–631. <https://doi.org/10.1016/j.neuroimage.2017.09.035>
- Goerke, U., Möller, H. E., Norris, D. G., & Schwarzbauer, C. (2005). A comparison of signal instability in 2D and 3D EPI resting-state fMRI. *NMR in Biomedicine: An International Journal Devoted to the Development and Application of Magnetic Resonance In vivo, 18*(8), 534–542. <https://doi.org/10.1002/nbm.987>
- Harrison, B. J., Pujol, J., Lopez-Sola, M., Hernandez-Ribas, R., Deus, J., Ortiz, H., Soriano-Mas, C., Yucel, M., Pantelis, C., & Cardoner, N. (2008). Consistency and functional specialization in the default mode brain network. *Proceedings of the National Academy of Sciences of the United States of America, 105*(28), 9781–9786. <https://doi.org/10.1073/pnas.0711791105>
- van den Heuvel, M. P., & Pol, H. E. H. (2010). Exploring the brain network: A review on resting-state fMRI functional connectivity. *European Neuropsychopharmacology, 20*(8), 519–534. <https://doi.org/10.1016/j.euroneuro.2010.03.008>
- Hodkinson, D. J., Krause, K., Khawaja, N., Renton, T. F., Huggins, J. P., Vennart, W., Thacker, M. A., Mehta, M. A., Zelaya, F. O., Williams, S. C. R., & Howard, M. A. (2013). Quantifying the test-retest

- reliability of cerebral blood flow measurements in a clinical model of on-going post-surgical pain: A study using pseudo-continuous arterial spin labelling. *Neuroimage-Clinical*, 3, 301–310. <https://doi.org/10.1016/j.nicl.2013.09.004>
- Jallouli, M., Zenni, M., Ben Mabrouk, A., & Mahjoub, M. A. (2021). Toward new multi-wavelets: Associated filters and algorithms. Part I: Theoretical framework and investigation of biomedical signals, ECG, and coronavirus cases. *Soft Computing*, 25(22), 14059–14079. <https://doi.org/10.1007/s00500-021-06217-y>
- Jia, X. Z., Zhao, N., Dong, H. M., Sun, J. W., Barton, M., Burciu, R., Carrière, N., Cerasa, A., Chen, B. Y., Chen, J., Coombes, S., Defebvre, L., Delmaire, C., Dujardin, K., Esposito, F., Fan, G.-G., Di Nardo, F., Feng, Y.-X., Fling, B. W., & Zang, Y.-F. (2021). Small P values may not yield robust findings: An example using REST-meta-PD. *Science Bulletin*, 66(21), 2148–2152. <https://doi.org/10.1016/j.scib.2021.06.007>
- Khullar, S., Michael, A., Correa, N., Adali, T., Baum, S. A., & Calhoun, V. D. (2011). Wavelet-based fMRI analysis: 3-D denoising, signal separation, and validation metrics. *NeuroImage*, 54(4), 2867–2884. <https://doi.org/10.1016/j.neuroimage.2010.10.063>
- Lefaucheur, J. P., Andre-Obadia, N., Antal, A., Ayache, S. S., Baeken, C., Benninger, D. H., Cantello, R. M., Cincotta, M., de Carvalho, M., De Ridder, D., Devanne, H., Di Lazzaro, V., Filipovic, S. R., Hummel, F. C., Jaaskelainen, S. K., Kimiskidis, V. K., Koch, G., Langguth, B., Nyffeler, T., ... Garcia-Larrea, L. (2014). Evidence-based guidelines on the therapeutic use of repetitive transcranial magnetic stimulation (rTMS). *Clinical Neurophysiology*, 125(11), 2150–2206. <https://doi.org/10.1016/j.clinph.2014.05.021>
- Lefaucheur, J. P., Aleman, A., Baeken, C., Benninger, D. H., Brunelin, J., Di Lazzaro, V., Filipovic, S. R., Grefkes, C., Hasan, A., Hummel, F. C., Jaaskelainen, S. K., Langguth, B., Leocani, L., Londero, A., Nardone, R., Nguyen, J. P., Nyffeler, T., Oliveira-Maia, A. J., Oliviero, A., ... Ziemann, U. (2020). Evidence-based guidelines on the therapeutic use of repetitive transcranial magnetic stimulation (rTMS): An update (2014–2018) (vol 131, pg 474, 2020). *Clinical Neurophysiology*, 131(5), 1168–1169. <https://doi.org/10.1016/j.clinph.2020.02.003>
- Lencer, R., Yao, L., Reilly, J. L., Keedy, S. K., McDowell, J. E., Keshavan, M. S., Pearlson, G. D., Tamminga, C. A., Gershon, E. S., Clementz, B. A., Lui, S., & Sweeney, J. A. (2019). Alterations in intrinsic fronto-thalamo-parietal connectivity are associated with cognitive control deficits in psychotic disorders. *Human Brain Mapping*, 40(1), 163–174. <https://doi.org/10.1002/hbm.24362>
- Lewis, L. D., Setsompop, K., Rosen, B. R., & Polimeni, J. R. (2016). Fast fMRI can detect oscillatory neural activity in humans. *Proceedings of the National Academy of Sciences of the United States of America*, 113(43), E6679–E6685. <https://doi.org/10.1073/pnas.1608117113>
- Li, Q. W., Zhu, W. J., Wen, X. M., Zang, Z. X., Da, Y. W., & Lu, J. (2022). Different sensorimotor mechanism in fast and slow progression amyotrophic lateral sclerosis. *Human Brain Mapping*, 43(5), 1710–1719. <https://doi.org/10.1002/hbm.25752>
- Lindquist, M. A., & Wager, T. D. (2007). Validity and power in hemodynamic response modeling: A comparison study and a new approach. *Human Brain Mapping*, 28(8), 764–784. <https://doi.org/10.1002/hbm.20310>
- Lio, P. (2003). Wavelets in bioinformatics and computational biology: State of art and perspectives. *Bioinformatics*, 19(1), 2–9. <https://doi.org/10.1093/bioinformatics/19.1.2>
- Liu, D., Dong, Z., Zuo, X., Wang, J., & Zang, Y. (2013). Eyes-open/eyes-closed dataset sharing for reproducibility evaluation of resting state fMRI data analysis methods. *Neuroinformatics*, 11(4), 469–476. <https://doi.org/10.1007/s12021-013-9187-0>
- Luo, F. F., Wang, J. B., Yuan, L. X., Zhou, Z. W., Xu, H., Ma, S. H., Zang, Y. F., & Zhang, M. (2020). Higher sensitivity and reproducibility of wavelet-based amplitude of resting-state fMRI. *Frontiers in Neuroscience*, 14, 224. <https://doi.org/10.3389/fnins.2020.00224>
- Malinen, S., Vartiainen, N., Hlushchuk, Y., Koskinen, M., Ramkumar, P., Forss, N., Kalso, E., & Hari, R. (2010). Aberrant temporal and spatial brain activity during rest in patients with chronic pain. *Proceedings of the National Academy of Sciences of the United States of America*, 107(14), 6493–6497. <https://doi.org/10.1073/pnas.1001504107>
- Otti, A., Guendel, H., Wohlschlagel, A., Zimmer, C., & Noll-Hussong, M. (2013). Frequency shifts in the anterior default mode network and the salience network in chronic pain disorder. *BMC Psychiatry*, 13, 84. <https://doi.org/10.1186/1471-244x-13-84>
- Perraudin, N., & Vandergheynst, P. (2017). Stationary signal processing on graphs. *IEEE Transactions on Signal Processing*, 65(13), 3462–3477. <https://doi.org/10.1109/TSP.2017.2690388>
- Qian, S. F., Wang, X. B., Qu, X. J., Zhang, P. W., Li, Q. Y., Wang, R. D., & Liu, D. Q. (2019). Links between the amplitude modulation of low-frequency spontaneous fluctuation across resting state conditions and thalamic functional connectivity. *Frontiers in Human Neuroscience*, 13. <https://doi.org/10.3389/fnhum.2019.00199>
- Rossi, S., Antal, A., Bestmann, S., Bikson, M., Brewer, C., Brockmoller, J., Carpenter, L. L., Cincotta, M., Chen, R., Daskalakis, J. D., Di Lazzaro, V., Fox, M. D., George, M. S., Gilbert, D., Kimiskidis, V. K., Koch, G., Ilmoniemi, R. J., Lefaucheur, J. P., Leocani, L., ... Hallett, M. (2021). Safety and recommendations for TMS use in healthy subjects and patient populations, with updates on training, ethical and regulatory issues: Expert guidelines. *Clinical Neurophysiology*, 132(1), 269–306. <https://doi.org/10.1016/j.clinph.2020.10.003>
- Shang, J., Bauml, J. G., Koutsouleris, N., Daamen, M., Baumann, N., Zimmer, C., Bartmann, P., Boecker, H., Wolke, D., & Sorg, C. (2018). Decreased BOLD fluctuations in lateral temporal cortices of premature born adults. *Human Brain Mapping*, 39(12), 4903–4912. <https://doi.org/10.1002/hbm.24332>
- Shang, J., Fisher, P., Bauml, J. G., Daannen, M., Baumann, N., Zimmer, C., Bartmann, P., Boecker, H., Wolke, D., Sorg, C., Koutsouleris, N., & Dwyer, D. B. (2019). A machine learning investigation of volumetric and functional MRI abnormalities in adults born preterm. *Human Brain Mapping*, 40(14), 4239–4252. <https://doi.org/10.1002/hbm.24698>
- Shrout, P. E., & Fleiss, J. L. (1979). Intraclass correlations: Uses in assessing rater reliability. *Psychological Bulletin*, 86(2), 420–428. <https://doi.org/10.1037/0033-2909.86.2.420>
- Sifuzzaman, M., Islam, M. R., & Ali, M. (2009). Application of wavelet transform and its advantages compared to Fourier transform. *Journal of Physical Science*, 13, 121–134. <http://inet.vidyasagar.ac.in:8080/jspui/handle/123456789/779>
- Torrence, C., & Compo, G. P. (1998). A practical guide to wavelet analysis. *Bulletin of the American Meteorological Society*, 79(1), 61–78. [https://doi.org/10.1175/1520-0477\(1998\)079<0061:APGTWA>2.0.CO;2](https://doi.org/10.1175/1520-0477(1998)079<0061:APGTWA>2.0.CO;2)
- Turner, J. A., Damaraju, E., Van Erp, T. G., Mathalon, D. H., Ford, J. M., Voyvodic, J., Mueller, B. A., Belger, A., Bustillo, J., & McEwen, S. C. (2013). A multi-site resting state fMRI study on the amplitude of low frequency fluctuations in schizophrenia. *Frontiers in Neuroscience*, 7, 137. <https://doi.org/10.3389/fnins.2013.00137>
- Vollmar, C., O'Muircheartaigh, J., Barker, G. J., Symms, M. R., Thompson, P., Kumari, V., Duncan, J. S., Richardson, M. P., & Koeppe, M. J. (2010). Identical, but not the same: Intra-site and inter-site reproducibility of fractional anisotropy measures on two 3.0T scanners. *NeuroImage*, 51(4), 1384–1394. <https://doi.org/10.1016/j.neuroimage.2010.03.046>
- van Vugt, M. K., Sederberg, P. B., & Kahana, M. J. (2007). Comparison of spectral analysis methods for characterizing brain oscillations. *Journal of Neuroscience Methods*, 162(1–2), 49–63. <https://doi.org/10.1016/j.jneumeth.2006.12.004>
- Wang, J., Zhang, Z. Q., Ji, G. J., Xu, Q., Huang, Y. B., Wang, Z. G., Jiao, Q., Yang, F., Zang, Y. F., Liao, W., & Lu, G. M. (2015). Frequency-specific alterations of local synchronization in idiopathic generalized epilepsy. *Medicine*, 94(32), e1374. <https://doi.org/10.1097/MD.0000000000001374>

- Wang, M., Yu, B. L., Luo, C. M., Fogelson, N., Zhang, J. J., Jin, Z. L., & Li, L. (2020). Evaluating the causal contribution of fronto-parietal cortices to the control of the bottom-up and top-down visual attention using fMRI-guided TMS. *Cortex*, *126*, 200–212. <https://doi.org/10.1016/j.cortex.2020.01.005>
- Wee, C. Y., Yap, P. T., Denny, K., Browndyke, J. N., Potter, G. G., Welsh-Bohmer, K. A., Wang, L. H., & Shen, D. G. (2012). Resting-state multi-Spectrum functional connectivity networks for identification of MCI patients. *PLoS One*, *7*(5), e37828. <https://doi.org/10.1371/journal.pone.0037828>
- Wei, J., Chen, T., Li, C. D., Liu, G. Y., Qiu, J., & Wei, D. T. (2018). Eyes-open and eyes-closed resting states with opposite brain activity in sensorimotor and occipital regions: Multidimensional evidences from machine learning perspective. *Frontiers in Human Neuroscience*, *12*, 422. <https://doi.org/10.3389/fnhum.2018.00422>
- Wilson, S. M., Bautista, A., Yen, M., Lauderdale, S., & Eriksson, D. K. (2017). Validity and reliability of four language mapping paradigms. *Neuroimage-Clinical*, *16*, 399–408. <https://doi.org/10.1016/j.nicl.2016.03.015>
- Yan, C., & Zang, Y. (2010). DPARSF: A MATLAB toolbox for "pipeline" data analysis of resting-state fMRI. *Frontiers in Systems Neuroscience*, *4*, 13. <https://doi.org/10.3389/fnsys.2010.00013>
- Yang, H., Long, X. Y., Yang, Y., Yan, H., Zhu, C. Z., Zhou, X. P., Zang, Y. F., & Gong, Q. Y. (2007). Amplitude of low frequency fluctuation within visual areas revealed by resting-state functional MRI. *NeuroImage*, *36*(1), 144–152. <https://doi.org/10.1016/j.neuroimage.2007.01.054>
- Yuan, B. K., Wang, J., Zang, Y. F., & Liu, D. Q. (2014). Amplitude differences in high-frequency fMRI signals between eyes open and eyes closed resting states. *Frontiers in Human Neuroscience*, *8*, 503. <https://doi.org/10.3389/fnhum.2014.00503>
- Yuan, L. X., Wang, J. B., Zhao, N., Li, Y. Y., Ma, Y., Liu, D. Q., He, H. J., Zhong, J. H., & Zang, Y. F. (2018). Intra- and inter-scanner reliability of scaled subprofile model of principal component analysis on ALFF in resting-state fMRI under eyes open and closed conditions. *Frontiers in Neuroscience*, *12*, 311. <https://doi.org/10.3389/fnins.2018.00311>
- Zang, Y. F., He, Y., Zhu, C. Z., Cao, Q. J., Sui, M. Q., Liang, M., Tian, L. X., Jiang, T. Z., & Wang, Y. F. (2007). Altered baseline brain activity in children with ADHD revealed by resting-state functional MRI. *Brain & Development*, *29*(2), 83–91. <https://doi.org/10.1016/j.braindev.2006.07.002>
- Zang, Y. F., Zuo, X. N., Milham, M., & Hallett, M. (2015). Toward a meta-analytic synthesis of the resting-state fMRI literature for clinical populations. *BioMed Research International*, *2015*, 1–3. <https://doi.org/10.1155/2015/435265>
- Zhang, H., Zhang, L., & Zang, Y. (2015). Fluctuation amplitude and local synchronization of brain activity in the ultra-low frequency band: An fMRI investigation of continuous feedback of finger force. *Brain Research*, *1629*, 104–112. <https://doi.org/10.1016/j.brainres.2015.10.023>
- Zhang, Z., Telesford, Q. K., Giusti, C., Lim, K. O., & Bassett, D. S. (2016). Choosing wavelet methods, filters, and lengths for functional brain network construction. *PLoS One*, *11*(6), e0157243. <https://doi.org/10.1371/journal.pone.0157243>
- Zhao, N., Yuan, L. X., Jia, X. Z., Zhou, X. F., Deng, X. P., He, H. J., Zhong, J., Wang, J., & Zang, Y. F. (2018). Intra- and inter-scanner reliability of voxel-wise whole-brain analytic metrics for resting state fMRI. *Frontiers in Neuroinformatics*, *12*, 54. <https://doi.org/10.3389/fninf.2018.00054>
- Zheng, X. Y., Sun, J. W., Lv, Y. T., Wang, M. X., Du, X. X., Jia, X. Z., & Ma, J. (2021). Frequency-specific alterations of the resting-state BOLD signals in nocturnal enuresis: An fMRI study. *Scientific Reports*, *11*(1), 12042. <https://doi.org/10.1038/s41598-021-90546-3>
- Zou, Q., Miao, X., Liu, D., Wang, D. J., Zhuo, Y., & Gao, J. H. (2015a). Reliability comparison of spontaneous brain activities between BOLD and CBF contrasts in eyes-open and eyes-closed resting states. *NeuroImage*, *121*, 91–105. <https://doi.org/10.1016/j.neuroimage.2015.07.044>
- Zou, Q. H., Yuan, B. K., Gu, H., Liu, D. Q., Wang, D. J. J., Gao, J. H., Yang, Y. H., & Zang, Y. F. (2015b). Detecting static and dynamic differences between eyes-closed and eyes-open resting states using ASL and BOLD fMRI. *PLoS One*, *10*(3), e0121757. <https://doi.org/10.1371/journal.pone.0121757>
- Zuo, X. N., & Xing, X. X. (2014). Test-retest reliabilities of resting-state fMRI measurements in human brain functional connectomics: A systems neuroscience perspective. *Neuroscience and Biobehavioral Reviews*, *45*, 100–118. <https://doi.org/10.1016/j.neubiorev.2014.05.009>
- Zuo, X. N., Di Martino, A., Kelly, C., Shehzad, Z. E., Gee, D. G., Klein, D. F., Castellanos, F. X., Biswal, B. B., & Milham, M. P. (2010a). The oscillating brain: Complex and reliable. *NeuroImage*, *49*(2), 1432–1445. <https://doi.org/10.1016/j.neuroimage.2009.09.037>
- Zuo, X. N., Kelly, C., Adelstein, J. S., Klein, D. F., Castellanos, F. X., & Milham, M. P. (2010b). Reliable intrinsic connectivity networks: Test-retest evaluation using ICA and dual regression approach. *NeuroImage*, *49*(3), 2163–2177. <https://doi.org/10.1016/j.neuroimage.2009.10.080>
- Zuo, X. N., Xu, T., & Milham, M. P. (2019). Harnessing reliability for neuroscience research. *Nature Human Behaviour*, *3*(8), 768–771. <https://doi.org/10.1038/s41562-019-0655-x>

SUPPORTING INFORMATION

Additional supporting information can be found online in the Supporting Information section at the end of this article.

How to cite this article: Yue, J., Zhao, N., Qiao, Y., Feng, Z.-J., Hu, Y.-S., Ge, Q., Zhang, T.-Q., Zhang, Z.-Q., Wang, J., & Zang, Y.-F. (2023). Higher reliability and validity of Wavelet-ALFF of resting-state fMRI: From multicenter database and application to rTMS modulation. *Human Brain Mapping*, *44*(3), 1105–1117. <https://doi.org/10.1002/hbm.26142>